J Neurophysiol 102: 774–785, 2009.
First published May 27, 2009; doi:10.1152/jn.91132.2008.

Cholinergic Responses and Intrinsic Membrane Properties of Developing Thalamic Parafascicular Neurons

Meijun Ye, Abdallah Hayar, and Edgar Garcia-Rill
Center for Translational Neuroscience, Department of Neurobiology and Developmental Sciences, University of Arkansas for Medical Sciences, Little Rock, Arkansas

Submitted 10 October 2008; accepted in final form 22 May 2009

Ye M, Hayar A, Garcia-Rill E. Cholinergic responses and intrinsic membrane properties of developing thalamic parafascicular neurons. *J Neurophysiol* 102: 774–785, 2009. First published May 27, 2009; doi:10.1152/jn.91132.2008. Parafascicular (Pf) neurons receive cholinergic input from the pedunculopontine nucleus (PPN), which is active during waking and REM sleep. There is a developmental decrease in REM sleep in humans between birth and puberty and 10–30 days in rat. Previous studies have established an increase in muscarinic and 5-HT1 serotonergic receptor–mediated inhibition and a transition from excitatory to inhibitory $GABA_A$ responses in the PPN during the developmental decrease in REM sleep. However, no studies have been conducted on the responses of Pf cells to the cholinergic input from the PPN during development, which is a major target of ascending cholinergic projections and may be an important mechanism for the generation of rhythmic oscillations in the cortex. Whole cell patch-clamp recordings were performed in 9- to 20-day-old rat Pf neurons in parasagittal slices, and responses to the cholinergic agonist carbachol (CAR) were determined. Three types of responses were identified: inhibitory (55.3%), excitatory (31.1%), and biphasic (fast inhibitory followed by slow excitatory, 6.8%), whereas 6.8% of cells showed no response. The proportion of CAR-inhibited Pf neurons increased with development. Experiments using cholinergic antagonists showed that M2 receptors mediated the inhibitory response, whereas excitatory modulation involved M1, nicotinic, and probably M3 or M5 receptors, and the biphasic response was caused by the activation of multiple types of muscarinic receptors. Compared with CAR-inhibited cells, CAR-excited Pf cells showed *1*) a decreased membrane time constant, *2*) higher density of hyperpolarization-activated channels (I_h), *3*) lower input resistance (R_{in}), *4*) lower action potential threshold, and *5*) shorter half-width duration of action potentials. Some Pf cells exhibited spikelets, and all were excited by CAR. During development, we observed decreases in I_h density, R_{in}, time constant, and action potential half-width. These results suggest that cholinergic modulation of Pf differentially affects separate populations, perhaps including electrically coupled cells. Pf cells tend to show decreased excitability and cholinergic activation during the developmental decrease in REM sleep.

INTRODUCTION

The parafascicular (Pf) and centrolateral (CL) nuclei are two major components of the intralamilar thalamus (ILT), which are traditionally considered as a major part of the "nonspecific" thalamocortical system. Recent studies, however, discovered that Pf cells are different from CL or typical "specific" thalamocortical (TC) neurons in morphology, electrophysiological properties, and some synaptic connections. Pf neurons have long, sparsely branching processes in their proximal dendrites instead of compact bushy primary dendrites like CL and TC cells (Deschenes et al. 1996a,b). TC neurons are present throughout the "specific" and some "nonspecific" thalamic nuclei and are bushy, multidendritic cells with stereotypical intrinsic properties, i.e., bistable states of tonic versus bursting patterns of activity caused by the ubiquitous incidence of low-threshold spike (LTS) currents (Llinas and Steriade 2006). This mechanism is considered essential to inducing cortical synchronization of high-frequency rhythms during waking and REM sleep (tonic pattern) and synchronization of low frequency rhythms during slow wave sleep (LTS + I_h oscillations). However, our previous electrophysiological studies showed that Pf cells exhibited reduced or absent LTS calcium currents (Phelan et al. 2005) compared with "specific" TC neurons (Jahnsen and Llinas 1984a; Llinas and Jahnsen 1982). It was recently reported that CL and Pf provide different patterned inputs to distinct striatal targets (Lacey et al. 2007). These findings suggest the possibility that Pf neurons may play a different role in the modulation of thalamocortical activity compared with CL or "specific" TC neurons.

As one of the targets of the cholinergic arm of the ascending reticular activating system (RAS), the ILT receives dense symmetrical and asymmetrical projections from the cholinergic pedunculopontine (PPN) and laterodorsal tegmental (LDT) nuclei (Capozzo et al. 2003; Erro et al. 1999; Kha et al. 2000; Kobayashi and Nakamura 2003), which participate in the modulation of cortical arousal, sleep-wake cycles, and sensory awareness (Van der Werf et al. 2002). In addition, Pf neurons were found to be involved in maintaining the state of consciousness and selective attention in primates (Minamimoto and Kimura 2002; Raeva 2006); they also receive vagal input and participate in the motor control as well as pain modulation (Ito and Craig 2005), presumably through their pathways to the striatum. In Parkinson's disease, degeneration is present in both PPN and ILT (including Pf) neurons (Henderson et al. 2000), suggesting a role for the PPN–Pf pathway in the control of voluntary movement; which was further supported by the observation of changes in firing frequency of Pf cells after lesions of the PPN and/or substantia nigra (Yan et al. 2008).

Cholinergic PPN neurons are most active during waking and REM sleep and contribute to the generation of fast thalamocortical oscillations (Steriade et al. 1990). Release of acetylcholine in the thalamus induced by PPN stimulation (Williams et al. 1994) blocks spindle oscillations and delta waves that appear in slow wave sleep (SWS), triggers the fast cortical oscillations of waking and REM sleep by depolarizing TC neurons (McCormick 1992), and hyperpolarizes reticular tha-

Address for reprint requests and other correspondence: E. Garcia-Rill, Ctr. for Translational Neuroscience, Dept. of Neurobiology and Developmental Sciences, Univ. of Arkansas for Medical Sciences, 4301 West Markham St., Slot 847, Little Rock, AR 72205 (E-mail: GarciaRillEdgar@uams.edu).

lamic neurons (nRt) (Hobson and Pace-Schott 2002; Steriade et al. 1993). Short lasting nicotinic and long-lasting muscarinic depolarizing responses induced by mesopontine cholinergic nucleus stimulation were intracellularly recorded in CL neurons (Curro Dossi et al. 1991). In the Pf, in addition to two types of excitation, long-lasting inhibition induced by PPN stimulation was observed in a subgroup of neurons using extracellular recordings (Capozzo et al. 2003). However, no further studies have been conducted describing cholinergic responses in Pf neurons.

The idea that the Pf performs different physiological functions from CL and typical "specific" TC neurons is supported by a wealth of data. To understand in detail the differential functions of the Pf, it is critical to explore the synaptic interactions of Pf neurons. We performed whole cell patch-clamp recordings on Pf neurons from 9- to 20-day-old rats, during which time REM sleep decreases sharply, to test their differential responses to cholinergic agents, with dual consideration of their intrinsic membrane properties and of their developmental changes.

METHODS

Slice preparation

Pups aged 9–20 days from adult timed-pregnant Sprague-Dawley rats (280–350 g) were anesthetized with ketamine (70 mg/kg, im) until tail pinch and corneal reflexes were absent. They were decapitated, and the brain was rapidly removed and blocked in cooled oxygenated (95% O_2-5% CO_2) sucrose artificial cerebrospinal fluid (sucrose-ACSF). The block of tissue was glued onto a stage, and 400-μm parasagittal slices containing the thalamus were cut with a Vibratome 1000 Plus with a 900R refrigeration system (Vibratome Instruments, St. Louis, MO) under cooled oxygenated sucrose-ACSF and allowed to equilibrate at room temperature in oxygenated ACSF for $\geq$1 h before recording. All animal use procedures were approved by the University of Arkansas for Medical Sciences Institutional Animal Care and Use Committee and comply with the ethical standards described in the National Institutes of Health guide. The ACSF consisted of (in mM) 117 NaCl, 4.7 KCl, 1.2 $MgSO_4$, 2.5 $CaCl_2$, 2.8 NaH_2PO_4, 24.9 $NaHCO_3$, and 11.5 glucose. The sucrose-ACSF was composed of (in mM) 233.7 sucrose, 26 $NaHCO_3$, 8 $MgCl_2$, 0.5 $CaCl_2$, 20 glucose, and 0.5 ascorbic acid.

Whole cell patch-clamp recordings

Whole cell patch-clamp recordings were acquired using borosilicate glass pipettes (with filament) with resistance of 8–12 MΩ, which were pulled on a Sutter P-87 puller (Sutter Instrument, Novato, CA) and filled with a solution containing (in mM) 124 K-gluconate, 10 phosphocreatine di tris salt, 10 HEPES, 0.2 EGTA, 4 MgATP, 0.3 Na_2GTP, and 0.5% neurobiotin. Osmolarity was adjusted to ~270–290 mOsm and pH to 7.4. Slices were recorded at 30°C while superfused (~1.5 ml/min) with oxygenated ACSF. Neurons were visualized using an upright microscope (Nikon FN1 with ×40 water immersion lens, ×1–2 magnifying turret, and Gibraltar platform; Nikon Instruments, Melville, NY) equipped for epifluorescence and near-infrared differential interference contrast optics. Only cells immediately posterior or anterior to the fasciculus retroflexus (fr) were recorded. All recordings were made using a Multiclamp 700B amplifier (low-pass filtered at 2 kHz) and a Digidata-1440A (digitized at 5 kHz) (Molecular Devices, Union City, CA). Bath-applied drugs were administered to the slice via a peristaltic pump (Cole-Parmer, Vernon Hills, IL) and a three-way valve system. To determine intrinsic membrane properties of cells, a series of depolarizing and hyperpolarizing steps were applied at resting membrane potential (RMP) in current-clamp mode (−100 to 60 pA, 20-pA step, 500 ms in duration) and at −55 mV in voltage-clamp mode (−105 to 15 mV, 15-mV step, 500 ms in duration).

Data analysis

Off-line analyses were performed using Clampfit 10 software (Molecular Devices). Only cells with action potential amplitude higher than 50 mV and stable resting membrane potential (if not spontaneously firing, more negative than −45 mV) were included in the statistical analysis. The following intrinsic membrane properties were characterized (Fig. 1): resting membrane potential (RMP, spontaneously firing cells were excluded), action potential (AP) threshold (determined by the AP that appeared in the depolarization *I-V* steps), AP amplitude, AP half-width duration, input resistance (R_{in}, calculated by measuring the instantaneous current in response to a hyperpolarization step from −55 to −105 mV), membrane time constant (tau, determined by fitting an exponential decay curve to the initial portion of a hyperpolarizing potential of about −40 mV induced by a negative current step), membrane capacitance, rebound inward current density (normalized to membrane capacitance, pA/pF; determined by a hyperpolarizing step from −55 to −105 mV under voltage clamp), hyperpolarization-activated cation I_h current density (determined in the same way as rebound current). Data, expressed as mean ± SE, were statistically analyzed using two-tail Student's *t*-test (Origin 7.0). Linear regression analyses were performed using Origin 7.0.

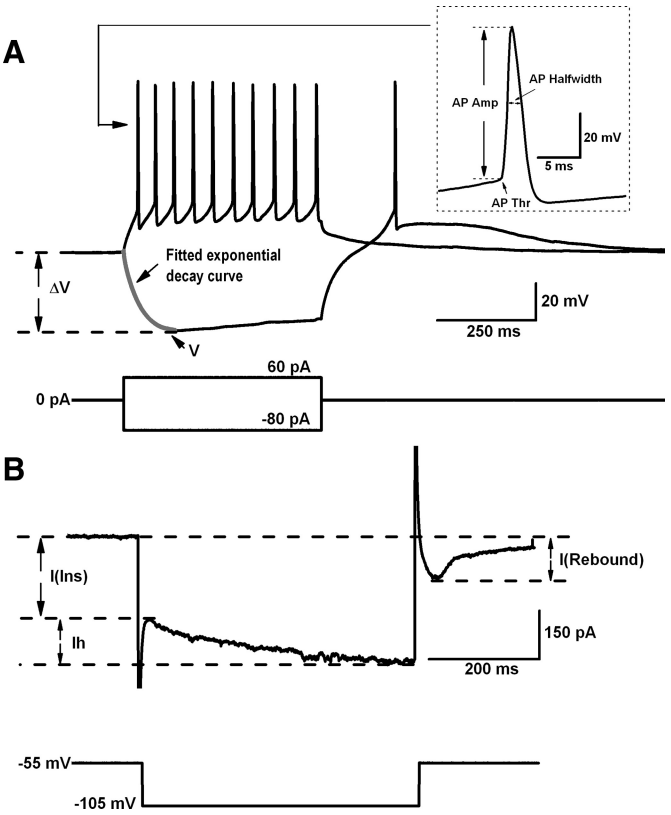

FIG. 1. Measurement of intrinsic membrane properties. *A*: representative *I-V* steps under current-clamp mode. Time constant (tau) was determined using the following equation: $V = -\Delta V \times e^{-t/tau}$. *B*: single *I-V* step under voltage-clamp mode. R_{in} = 50 mV/*I*(Ins). Membrane capacitance (*C*) = tau/R_{in}. Normalized rebound current (or I_h current) = *I*(Rebound) [or I_h]/*C*. AP, action potential; Amp, amplitude; Thr, threshold; *I*(ins), instantaneous current.

Drugs

Drugs used in this study included the voltage-gated sodium channel blocker TTX (1 μM), nonselective cholinergic receptor agonist carbachol (CAR, 50 μM), competitive nonselective muscarinic cholinergic receptor (mAChR) antagonist atropine (ATR, 10 μM), noncompetitive neuronal nAChR antagonist mecamylamine (MEC, 10 μM), selective M2 AChR antagonist methoctramine (MTO, 2 μM), selective M1 AChR antagonist pirenzepine (PRZ, 10 μM), selective NMDA receptor antagonist 2-amino-5-phosphonovaleric acid (APV, 10 μM), competitive AMPA/kainate glutamate receptor antagonist 6-cyano-7-nitroquinoxaline-2,3-dione (CNQX, 10 μM), specific GABAa receptor antagonist gabazine (GBZ, 10 μM), GABAb receptor antagonist CGP55845 (CGP, 10 μM), glycine receptor antagonist strychnine (STR, 10 μM), α2-adrenergic receptor antagonist yohimbine hydrochloride (YOH, 2 μM), selective 5-HT1a receptor antagonist WAY-100635 maleate salt (WAY, 10 μM), selective 5-HT2 antagonist ketanserin tartrate salt (KET, 10 μM), and inward rectifying potassium current blocker $BaCl_2$ (Ba^{2+}, 1 mM). All drugs, including components used in ACSF, sucrose-ACSF, and intracellular solution, were purchased from Sigma (St. Louis, MO), except for CGP55845 and TTX, which were purchased from Tocris Bioscience (Ellisville, MO), and neurobiotin, which was from Vector Laboratories (Burlingame, CA).

Histology

All cells included in statistical analyses were located immediately posterior or anterior to the fr (Fig. 2*A*). After recording, slices were fixed for 1 h in 4% paraformaldehyde and stored in PBS for further immunolabeling with goat polyclonal anti-biotin conjugated to Cy2 (Fig. 2*B*).

RESULTS

Postsynaptic responses of Pf neurons to CAR

Whole cell voltage-clamp recordings were conducted to determine the effects of the nonselective cholinergic agonist CAR, as well as specific cholinergic antagonists, which were applied by bath for 3 min. Membrane potential was held at −55 mV. Every 10 or 20 s, a voltage step to −100 or −95 mV was applied for 500 ms to determine input resistance (R_{in}), followed by a 1,000-ms ramp from −100 to −30 mV or from −95 to −25 mV to determine the reversal potential of the activated currents. We tested CAR on 103 Pf neurons from 9- to 20-day-old rats. An outward current, indicating an inhibitory response, was induced in 57 (55.3%) neurons, whereas 32 (31.1%) neurons exhibited an inward current, indicating an excitatory response induced by CAR. Seven cells (6.8%) responded to CAR by a fast outward current followed by an inward current, and seven other cells (6.8%) showed no response to CAR.

To determine whether presynaptic neurotransmitter release accounted for the responses observed, we tested the voltage-gated sodium channel blocker TTX (1 μM) on 54 cells (18 excited cells, 32 inhibited cells, and 4 cells with biphasic responses), as well as excitatory (CNQX 10 μM and APV 10 μM) or inhibitory receptor blockers (GBZ 10 μM, CGP55845 10 μM, STR 10 μM, KET 10 μM, YOH 2 μM, and WAY 10 μM) on nine Pf neurons (4 excited and 5 inhibited neurons). We found that pretreatment with TTX decreased the amplitude of outward currents to 58 ± 6% of the responses to CAR alone ($n = 32$, $P < 0.0001$, paired *t*-test), whereas the amplitude of inward currents was reduced to 87 ± 10% of the responses to CAR alone ($n = 18$, $P < 0.01$, paired *t*-test). Excitatory or inhibitory receptor blockers reduced or diminished excitatory or inhibitory postsynaptic currents (EPSCs or IPSCs), but had little effect on the amplitude of CAR-induced prolonged inward or outward currents (Fig. 3, *E* and *F*; for CAR-excited cells, 31 ± 4 pA in the presence of TTX alone, 26 ± 7 pA with antagonists: $n = 4$, $P = 0.25$; for CAR-inhibited cells, 14 ± 1 pA with TTX alone, 13 ± 3 pA with antagonists: $n = 5$, $P = 0.70$; paired *t*-test). To identify whether the desensitization of receptors was responsible for the decrease of CAR-induced responses, we tested the effects of repetitive application of CAR (4 applications of 3-min duration separated by 15-min intervals). For CAR-excited cells, compared with the initial responses, responses to applications 2 through 4 decreased to 70 ± 12 ($n = 4$, $P = 0.22$ vs. 1st application; paired *t*-test), 60 ± 14 ($n = 4$, $P = 0.39$ vs. 2nd application; paired *t*-test), and 52 ± 6% ($n = 4$, $P = 0.39$ vs. 3rd application; paired *t*-test; Fig. 3, *A* and *C*). For CAR-inhibited cells, subsequent responses were reduced to 61 ± 8 ($n = 4$, $P < 0.05$ vs. 1st application; paired *t*-test), 61 ± 8, and 57 ± 11% ($n = 4$, $P = 0.39$ vs. 3rd application; paired *t*-test; Fig. 3, *B* and *D*). The second responses showed a large decrease in amplitude; however, the third and fourth responses were only slightly further reduced. CAR-inhibited cells responded with ≥33.3% of the amplitude of the initial responses to the fourth CAR application, and CAR-excited cells responded with ≥40% of the amplitude of the initial responses to the fourth CAR application. These data indicated that the prolonged inward or outward currents induced by CAR were mostly caused by the activation of postsynaptic cholinergic receptors. Moreover, repetitive responses to CAR exhibited tachyphilaxis,

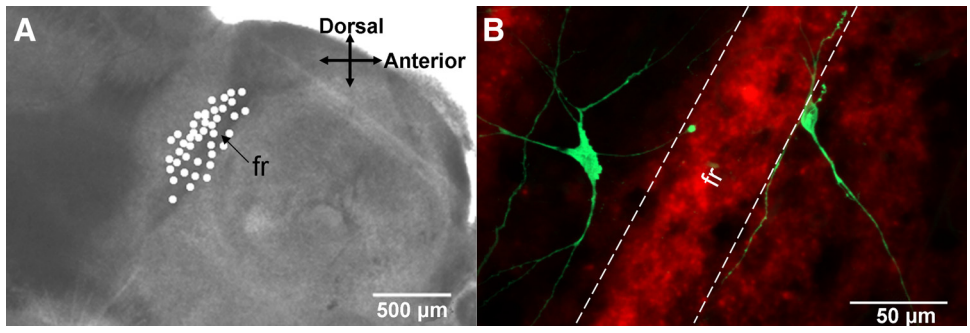

FIG. 2. Localization and morphology of parafascicular (Pf) neurons. *A*: location of some of the recorded Pf cells immediately posterior or anterior to the fasciculus retroflexus reconstructed on a 400-μm parasagittal thalamic section. *B*: 2-dimensional confocal image of 2 17-day Pf neurons identified by intracellular neurobiotin conjugated to Cy2 labeling from a single frame. The cell posterior to the fr was inhibited by carbachol (CAR) application and had a capacitance of 106 pF. The neuron anterior to the fr showed no response to CAR and had a capacitance of 101 pF. Note the long sparsely branching processes of both neurons. The morphology of CAR-excited and -inhibited and nonresponsive cells was similar.

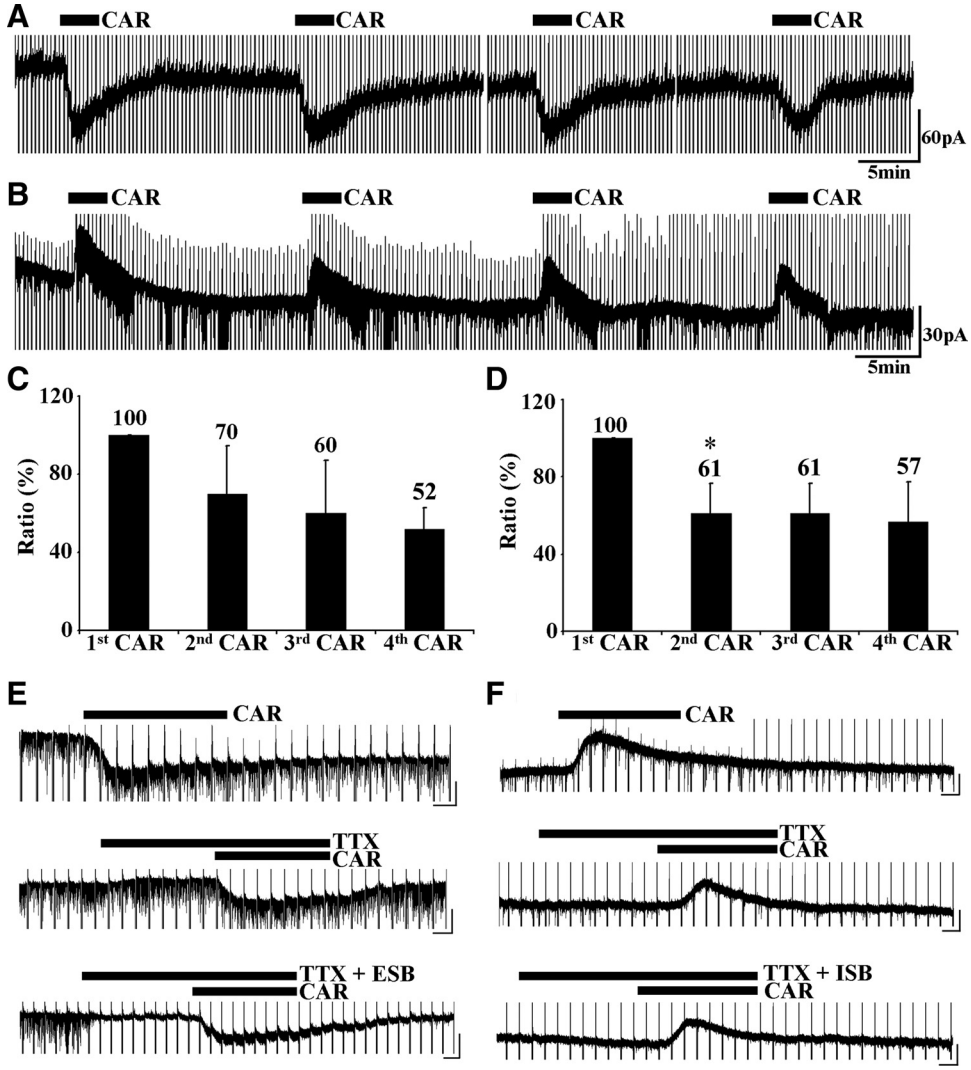

FIG. 3. Responses of Pf neurons to CAR or cholinergic antagonists were via postsynaptic receptors. *A*: repetitive application of CAR produced a slight rundown of the inward current induced by CAR. The 1st application of CAR induced a 60-pA inward current, with as much as 40 pA induced by the 4th application. *B*: outward current triggered by CAR decreased slightly with repetitive application. *C*: summary graph showing the average rundown ratio of the inward current produced by repetitive application of CAR. Baseline was the amplitude of the 1st response. *D*: summary graph showing the average rundown ratio of the outward current caused by repetitive application of CAR. *E*: TTX and excitatory synaptic blockers (ESBs) (ESB: CNQX and APV) failed to block the inward current induced by CAR. Top recording shows the effect of CAR alone, with a 50-pA inward current being induced. In the presence of TTX, the CAR-induced inward current decreased to 35 pA. ESBs did not affect the inward current, but excitatory postsynaptic currents (EPSCs) were blocked. *F*: the outward current produced by CAR was not blocked by TTX or by inhibitory synaptic blockers (ISB: GBZ + CGP + STR + YOH + WAY + KET). Black bars indicate the period when neuroactive agents were applied. Horizontal scale bars in *E* and *F* are 500 ms. Vertical scales in *E* are 40 pA and in *F* are 15 pA.

but a significant response was produced even during the fourth CAR application.

Inhibitory cholinergic responses of Pf cells were caused by the activation of M2 muscarinic receptors

CAR induced 25 ± 2-pA outward current (n = 57) in the absence of TTX in Pf cells. In the presence of TTX, the outward current induced by subsequent administration of CAR was 15 ± 1 pA (n = 32) and was blocked by pretreatment with the M2 muscarinic receptor antagonist, methoctramine (MTO, 2 μM; Fig. 4; n = 16). Analysis of current responses to hyperpolarizing pulses showed a decrease in R_{in} by CAR with or without TTX, which was blocked by MTO. The current-voltage (*I-V*) relationship was obtained using the voltage-ramp protocol, which was analyzed at the peak CAR effect and in control conditions. Subtracting the current ramp at the peak of the CAR effect from the control ramp, as indicated in Fig. 4, *C* and *F*, showed that the outward current generated by CAR reversed at −69 ± 1 mV (n = 32; when adjusted to a 9- to 12-mV junction potential, it was approximately −78 to −81 mV) in the presence of TTX. Subtraction of the current ramp obtained during CAR administration from that obtained in MTO showed a trace superimposed on the voltage axis at 0 pA (Fig. 4*C*; n = 13), indicating no activated current. For 3 of 16 cells, in the presence of MTO, an inward current was still evident after subsequent application of CAR, which was blocked by the nicotinic receptor antagonist, mecamylamine (MEC, 10 μM; data not shown).

In addition to MTO, the inwardly rectifying potassium channel blocker, barium (Ba^{2+}, 1 mM), was tested (Fig. 4, *D–F*; n = 6). In the presence of Ba^{2+}, the amplitude of outward currents activated by CAR decreased to 5 ± 1 pA (n = 6, $P < 0.05$, paired t-test; vs. in the presence of TTX). Ba^{2+} alone slightly increased R_{in}, but significantly reduced the R_{in} decrease produced by CAR (Fig. 4*E*). These data indicate that the inhibitory outward current induced by CAR in Pf cells was most likely caused by the activation of M2 receptors, mainly via the opening of inwardly rectifying potassium channels, although the possibility of involvement of other ion channels cannot be excluded.

Excitatory cholinergic responses of Pf neurons involved M1, nAChR, and perhaps M3 or M5 receptors

CAR induced an inward current of 33 ± 4 pA (n = 32) in the absence of TTX. In the presence of TTX, the inward current induced by subsequent administration of CAR was 24 ± 4 pA (n = 18). The CAR-induced inward currents in Pf neurons

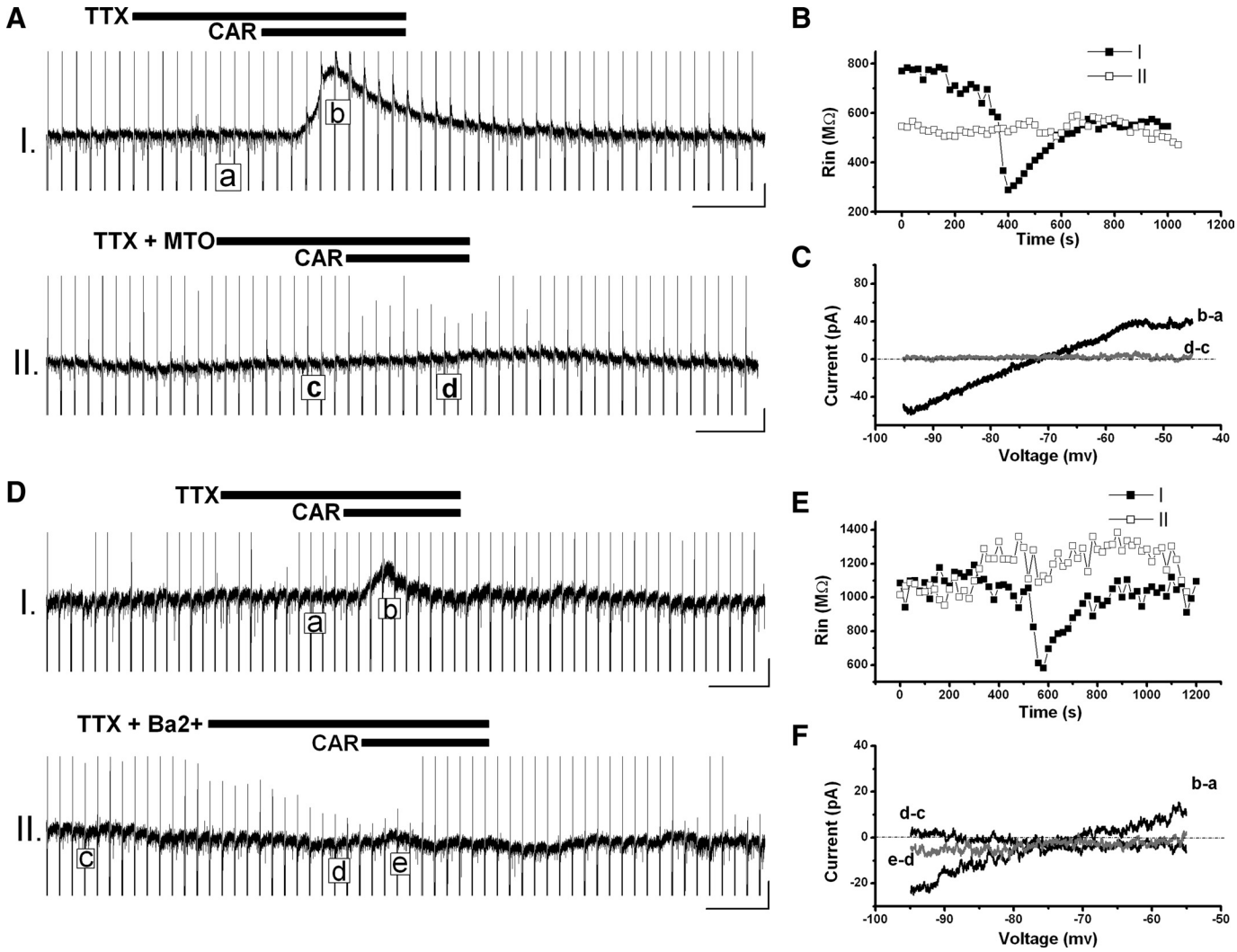

FIG. 4. Outward current induced by CAR was caused by the activation of M2 receptors mainly via opening the inwardly rectifying potassium channels in the Pf. *A*: outward current induced by CAR in the presence of TTX (recording I) was blocked by pretreatment with methoctramine (MTO) (recording II) in this Pf neuron. *B*: input resistance (R_{in}) change during recordings in *A*. CAR decreased the R_{in} from ~700 to ~300 MΩ in the presence of TTX, which recovered to ~600 MΩ after wash with artificial cerebrospinal fluid (ACSF) (recording I). In the presence of MTO, CAR failed to decrease R_{in} (recording II). *C*: *I-V* relationship obtained in recordings (*A*). Subtraction of current ramp at the peak CAR effect (*b*) from that in control condition (*a*) showed that the CAR-induced outward current reversed at approximately −72 mV ($b - a$); however, in the presence of MTO, subtraction of control from CAR ($d - c$) showed no deviation from the voltage axis at 0 pA, suggesting that no current was activated. *D*: the CAR-induced outward current in the presence of TTX (recording I) was significantly reduced by Ba^{2+} (recording II). *E*: R_{in} change during recordings in *D*. Note that Ba^{2+} slightly increased R_{in} and significantly reduced the R_{in} decrease induced by CAR. *F*: subtractions of current ramps in different conditions indicated that the CAR-induced outward current reversed at approximately −72 mV in the presence of TTX ($b - a$), Ba^{2+} induced a small inward current reversing at approximately −87 mV ($d - c$), and almost completely blocked the current induced by CAR ($e - d$). Black bars show the period when drugs were applied. Horizontal scale bars are 100 s, and vertical bars are 10 pA.

exhibited a wide range of reversal potentials and were associated with a small decrease in R_{in} in the presence of TTX. These results indicate that a variety of ion channels may be involved in the CAR-induced inward current in Pf neurons. Further experiments ($n = 14$) in the presence of TTX together with the M1 muscarinic receptor antagonist, pirenzepine (PRZ, 10 μM), and the nicotinic receptor antagonist, mecamylamine (MEC, 10 μM), suggested that M1, nAChR, and probably M3 or M5 receptors participated in the excitatory responses (Fig. 5). For some of these cells, the CAR-induced inward current was blocked by pretreatment with PRZ ($n = 6/14$). However, in 8 of 14 cells, CAR-induced inward currents exhibited multiple phases having different kinetics: fast short, fast medium, and/or slow long (Fig. 5). In four of them, the previous addition of MEC blocked the fast short inward current, whereas the fast medium phase was blocked by PRZ (Fig. 5*A*). In the other four cells, a slow and long inward current persisted even with co-pretreatment of PRZ and MEC (Fig. 5*B*). These data indicate that Pf neurons may have differential expression of single or multiple excitatory cholinergic receptors; among them, nicotinic receptors may be responsible for the fast and short CAR-generated inward current, M1 and/or M3 receptors may be involved in the fast and medium duration current, and the slow and long duration inward current could be caused by the activation of M3 and/or M5 receptors.

Biphasic cholinergic responses in the Pf were induced by activation of mAChRs

In the absence of TTX, a fast outward current followed by a prolonged inward current was activated by CAR in seven

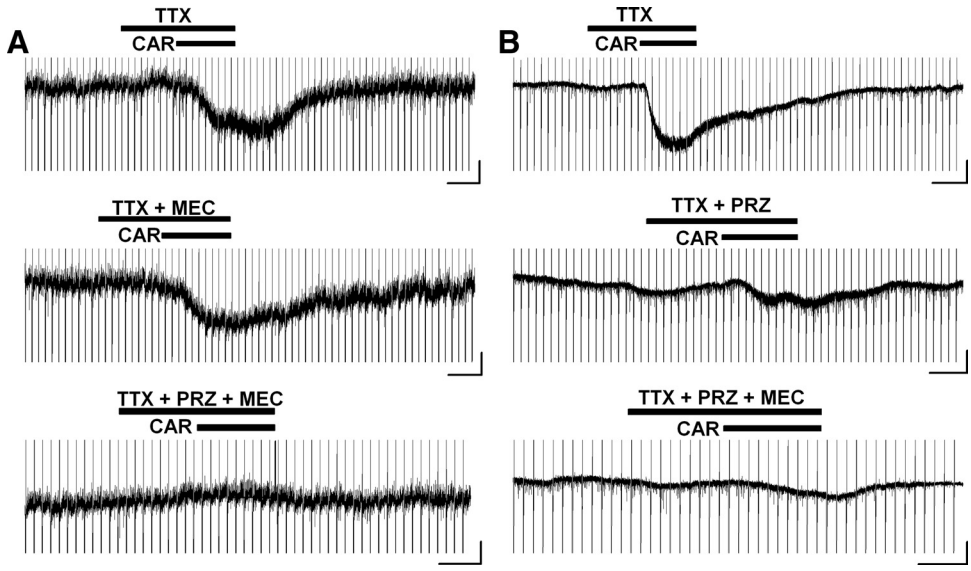

FIG. 5. Excitatory inward currents induced by CAR involved the activation of M1, nicotinic cholinergic receptor and probably M3 or M5 receptors in the Pf. *A*: CAR-induced inward currents were not blocked by mecamylamine (MEC) alone but were blocked during co-pretreatment with pirenzepine (PRZ) and MEC. Note the 2 phases of inward current in the top recording, whereas only 1 phase was present in the 2nd recording. *B*: inward currents induced by CAR were partially blocked by PRZ or co-application of PRZ and MEC. Note the 2 phases in the 2nd recording. Black bars show the period during which neuroagents were applied, and scale bars are 100 s and 20 pA for the horizontal and vertical axes, respectively.

(6.8%) Pf neurons. The amplitude of the outward current was 15 ± 4 pA and that of the inward current was 17 ± 3 pA. Subtracting the current ramp induced by CAR at the peak inhibitory/excitatory effect from the control ramp (Fig. 6*B*) showed that the outward current reversed at −62 ± 2 mV and the inward current reversed at a potential higher than −45 mV. Pretreatment with TTX before the application of CAR reduced the amplitude of these effects, especially of the outward current, but was not able to block it entirely; a 4 ± 1-pA outward current and a 16 ± 2-pA inward current persisted. In the presence of TTX, administration of atropine (ATR, 10 μM), a nonselective muscarinic receptor antagonist, completely blocked the biphasic response to CAR (Fig. 6). These data suggest that the biphasic cholinergic response in the Pf may be caused by the activation of multiple types of mAChRs through opening of different ion channels with distinct activation dynamics.

Distinct properties of Pf neurons with differential cholinergic responses

The intrinsic membrane properties of Pf neurons were characterized under voltage and/or current-clamp modes. Distinct membrane properties were identified in groups with different cholinergic responses (Table 1). Eighty-three percent (n = 47/57) of CAR-inhibited Pf neurons, 81% (n = 26/32) of excited cells, and 86% (n = 6/7) of cells with biphasic cholinergic responses showed rebound currents, which can be caused by the activation of either the low threshold calcium current (LTS) or the hyperpolarization-activated inward (I_h) current, or both. I_h currents were present in 44% (n = 25/57) of inhibited cells, 84% of excited cells (n = 27/32), and 29% (n = 2/7) of biphasically responding cells. Six neurons exhibited spontaneous or CAR-induced spikelets, and all of them were excited by CAR. Interestingly, the frequency of spikelets in the presence of CAR was in the

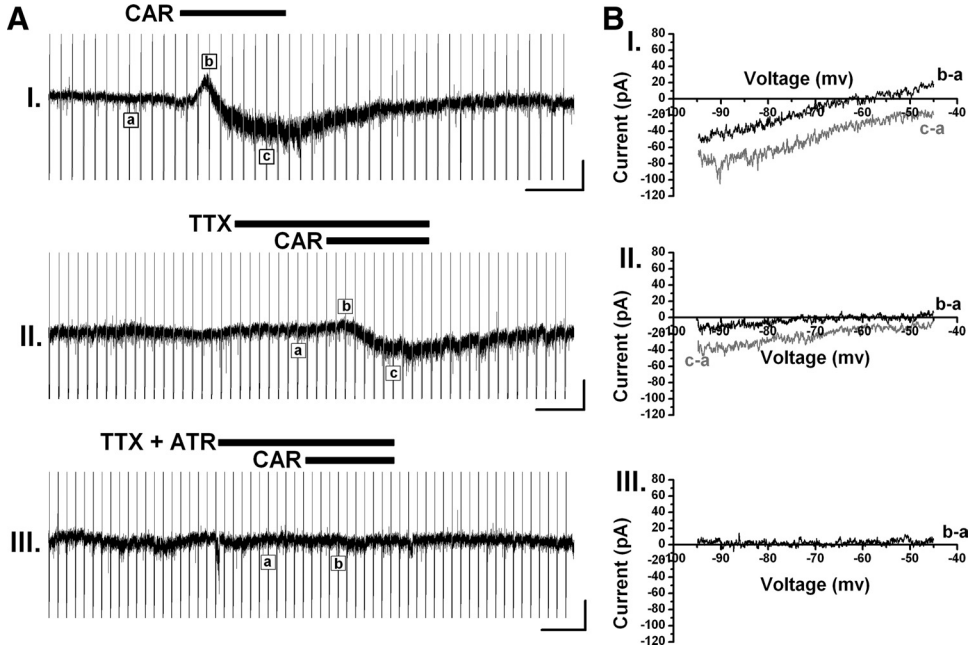

FIG. 6. Biphasic cholinergic response of the Pf was induced by the activation of muscarinic cholinergic receptors (mAChRs). *A*: a fast outward current followed by a slow inward current was produced by the administration of CAR with or without TTX, which was blocked by atropine (ATR). *B*: *I-V* relationship obtained from subtraction of current ramps at the peak CAR effect from that in control conditions. Recording I: *I-V* curve of (b − a) showed that the reversal potential of the CAR-activated fast outward current was approximately −62 mV and that of (c − a) suggested a reversal potential higher than −45 mV for the CAR-induced inward current. Recording (II): in the presence of TTX, the reversal potential did not show remarkable changes compared with that in recording I. Recording III: *I-V* relationship of (b − a) showed a parallel line to the voltage-axis at ~0 pA, indicating no current was activated. Black bars show the period when drugs were applied. Vertical scale bars are 20 pA and horizontal bars are 100 s.

TABLE 1. *Differential intrinsic membrane properties of pf neurons with distinct cholinergic responses*

	CAR-Inhibited (n = 57)	CAR-Excited (n = 32)	CAR-Biphasic (n = 7)	CAR-None (n = 7)	Total (n = 103)
Spontaneous Firing, n	10	5	2	2	19
Spikelets, n		6			6
Time Constant, ms	52.94 ± 3.71	28.54 ± 2.73‡	22.27 ± 2.54**	28.83 ± 2.44	41.65 ± 2.56
Capacitance, pF	83.94 ± 4.62	95.61 ± 7.56	57.77 ± 7.86§	95.8 ± 7.94	86.53 ± 3.63
Rebound I/C, pA/pF	0.36 ± 0.1	1.07 ± 0.27†	3.24 ± 2.45**	0.96 ± 0.39	0.82 ± 0.2
I_h/C, pA/pF	0.08 ± 0.03	0.71 ± 0.15‡	0.39 ± 0.34*	0.39 ± 0.27	0.32 ± 0.06
RMP, mv	−49.22 ± 0.85	−51.46 ± 1.07	−54.67 ± 3.39§,**	−52.6 ± 0.8	−50.44 ± 0.62
R_{in}, MΩ	702.02 ± 53.77	329.77 ± 38.60‡	492.97 ± 164.49	314.95 ± 37.17	545.86 ± 38.01
Amplitude of AP, mv	54 ± 0.74	53.5 ± 1.1	59 ± 4.39	55.2 ± 0.97	54.2 ± 0.61
Threshold of AP, mv	−28.9 ± 0.60	−34.27 ± 0.76‡	−34 ± 1.18*	−32.67 ± 1.65	−31.2 ± 0.51
AP halfwidth, ms	2.43 ± 0.18	1.75 ± 0.13†	1.5 ± 0.28	1.83 ± 0.26	2.11 ± 0.11

Values are means ± SE. †$P < 0.01$; ‡$P < 0.001$, independent t-test between CAR-inhibited and excited groups. §$P < 0.05$; independent t-test between CAR-excited and biphasic responding Pf neurons. *$P < 0.05$, **$P < 0.01$; independent t-test between CAR-inhibited and biphasic responding groups. Pf, parafascicular; CAR, carbachol.

theta range (4–8 Hz; Fig. 7, *A* and *B*). No major differences in morphology were identified following immunohistochemical processing in 42 of 103 cells between CAR-inhibited and -excited Pf neurons; however, 62% of inhibited and 92% of excited Pf cells were located posterior to the fr.

Table 1 shows the results of an independent t-test between CAR-inhibited and -excited Pf neurons, which showed that the CAR-excited cells had *1*) shorter time constant (ms), *2*) higher density of rebound currents (pA/pF), *3*) higher density of I_h currents (pA/pF), *4*) lower input resistance (MΩ), *5*) lower action potential threshold (mV), and *6*) shorter half-width duration of action potentials (ms). Representative records from each group are shown in Fig. 7, *C–F*. Pf cells with biphasic responses to CAR were more similar to the excited neurons

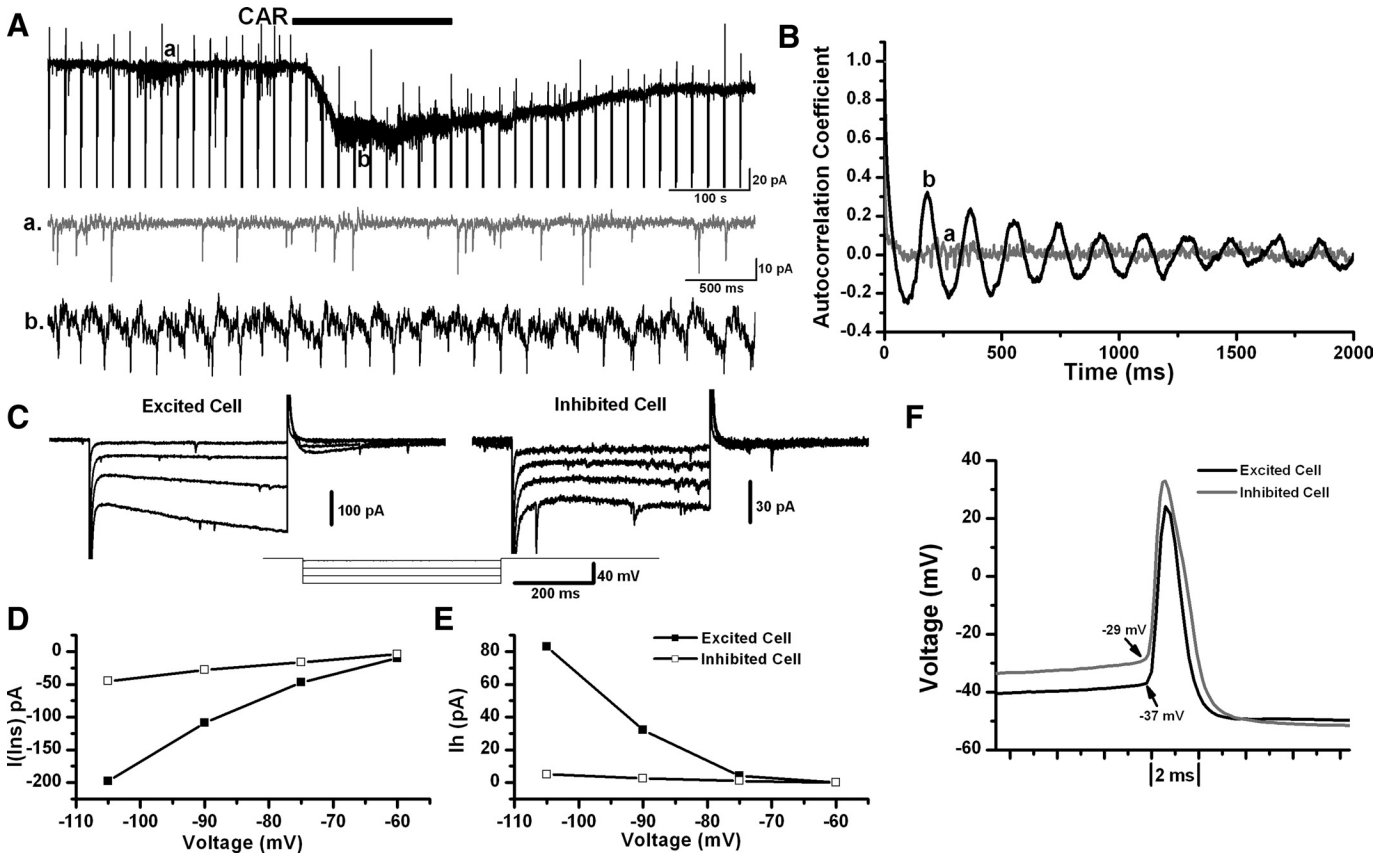

FIG. 7. Membrane property records of Pf neurons with differential cholinergic responses. *A*: CAR induced an inward current in this Pf neuron, as well as rhythmic spikelets. *a* and *b* are shorter time scale representative records in controls (in ACSF) and during CAR application, showing the occurrence of EPSCs and spikelets, respectively. *B*: autocorrelograms of records shown in *a* and *b* indicated that spikelets occurred rhythmically at a frequency ~5 Hz. *C*: representative *I-V* steps under voltage-clamp mode from 2 12-day-old Pf cells, 1 of them was excited by CAR, and the other was inhibited. *D*: relationship between voltage and instantaneous current [*I*(ins)] of 2 representative cells in *C*. Although a small rectifying current was present, the excited cell still showed a higher slope, indicating a lower R_{in}, whereas the inhibited cell exhibited a lower slope, indicating a higher R_{in}. *E*: relationship between voltage and I_h for the 2 cells shown in *C*. *F*: action potentials of 2 12-day-old representative Pf cells with different cholinergic responses. The excited cell showed a lower action potential threshold and a shorter half-width.

than the inhibited cells, except that the biphasic responding cells showed lower membrane capacitance, suggesting a smaller cell size and lower RMP. Membrane properties of Pf neurons exhibiting no responses to CAR were not compared with other groups because these cells might have been either unhealthy or had no functional cholinergic receptors. The above data suggested that the cholinergic agonist CAR differentially affected separate populations of Pf cells.

Development of Pf neurons and cholinergic responses

To determine whether the cholinergic responses of Pf cells, as well as their intrinsic membrane properties, change with development, neurons responding to CAR application were divided into four age groups (9–11, 12–14, 15–17, and 18–20 days). The proportion of Pf cells with different cholinergic responses were plotted across age (Fig. 8*A*), which showed a decrease in the proportion of CAR-excited cells and an increase in the inhibited neurons with development. A small percentage of cells showed fast inhibitory followed by excitatory biphasic responses starting at day 13, but it was uncertain whether the biphasic response increased with development. However, irrespective of cholinergic responses, Pf neurons showed a general developmental decrease in I_h current density (linear regression, $R = -0.29$, $P < 0.05$), in the proportion of neurons with I_h current, in R_{in} ($R = -0.28$, $P < 0.05$), and in AP half-width duration ($R = -0.48$, $P < 0.0001$). A significant developmental decrease in R_{in} ($R = -0.59$, $P < 0.0001$), AP half-width duration ($R = -0.66$, $P < 0.0001$), and in the proportion of neurons with I_h, as well as a nonsignificant developmental decrease in I_h density ($R = -0.11$, $P = 0.62$), was observed in CAR-inhibited neurons. However, CAR-excited cells showed an increase in the proportion of neurons with I_h and a significant developmental decrease in I_h density ($R = -0.48$, $P < 0.05$) and AP half-width duration ($R = -0.45$, $P < 0.05$) and a nonsignificant decrease in R_{in} ($R = -0.08$, $P = 0.68$). The proportion of cells showing spontaneous or CAR-induced spikelets showed a tendency to decrease with age. The developmental change in cholinergic responses suggests that the excitation of Pf neurons tends to decrease with development.

DISCUSSION

We identified three types of postsynaptic cholinergic responses in Pf neurons that involve different types of receptors. We found that Pf cells that responded differentially to the cholinergic agonist CAR had distinct intrinsic membrane properties. Moreover, cholinergic responses, as well as membrane properties, of Pf neurons, changed with development.

Cellular mechanisms of functional postsynaptic cholinergic receptors in the Pf

In this study, direct postsynaptic cholinergic responses of Pf neurons were determined in the presence of TTX and noncholinergic inhibitory/excitatory receptor antagonists. TTX apparently reduced the amplitude of CAR-induced outward and inward currents; therefore the blockade of persistent sodium currents may play a role in the reduction of responses. It is possible, because of inadequate space clamp in whole cell recordings, that the membrane potential in remote dendrites was probably not held at the same level as the soma and would respond to CAR by a relatively larger depolarization or hyperpolarization. This in turn changes the state of persistent sodium currents and contributes to an enhanced current recorded in the soma. However, the extent of the involvement of persistent sodium current in the cholinergic responses is unlikely to be

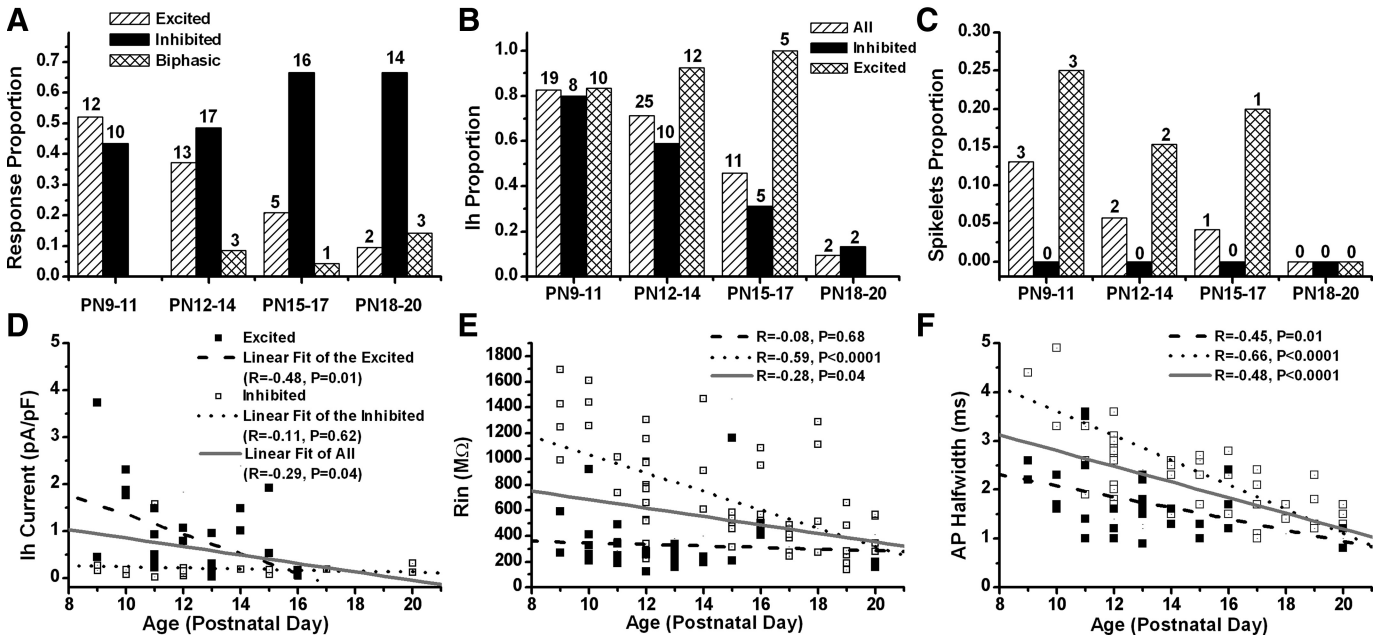

FIG. 8. Development of cholinergic responses and intrinsic membrane properties of Pf neurons. *A*: proportion of Pf cells with different cholinergic responses changed with development. A decrease in the proportion of CAR-excited neurons and an increase in inhibited cells were found. Biphasic cholinergic response appeared in the 12- to 14-day group. *B* and *C*: developmental changes in the proportion of Pf neurons with Ih and spontaneous or CAR-induced spikelets. Numbers above each column indicate the cell number of cells. *D–F*: scatter plots of the developmental changes of I_h, R_{in}, and AP half-width. Straight lines represent the corresponding linear regression fits for each group of cells.

significant, because the proportion of the decrease of cholinergic response by TTX was similar after repetitive CAR application in the absence of TTX, so that we assume that the reduction was more likely caused by tachyphilaxis. Therefore the absence of significant effects of TTX and noncholinergic inhibitory/excitatory receptor antagonists on the prolonged inward and outward currents induced by CAR strongly suggests that CAR-induced responses were caused by the direct activation of postsynaptic cholinergic receptors.

The CAR-induced outward current in the Pf seems to be mediated by activation of M2 receptors and subsequent increase in K^+ conductance, which was associated with a large decrease in R_{in}. This result is in line with early studies in other thalamic nuclei in the guinea pig and cat (McCormick and Prince 1987). The reversal potential of the CAR-induced outward current was approximately −78 to −81 mV, which is ~5 mV higher than −85 mV, the potassium equilibrium potential calculated from our extra- and intracellular solutions using the Nernst equation (T = 303 K, $[K^+]_o$ = 4.69 mM, $[K^+]_i$ = 124 mM). This small difference could be caused by the possible involvement of other ion channels. It has been reported that Ca^{2+} currents can be inhibited by activation of M2 receptors in other nuclei (Allen and Brown 1993; Endoh 2007). Because Ba^{2+} was not able to completely block the CAR-induced outward current, and the Ca^{2+} current activated by the ramp was decreased by CAR (preliminary findings), we suspect that Ca^{2+} channels may at least partially participate in the M2 receptor-mediated inhibitory cholinergic responses in the Pf.

The excitatory cholinergic response of Pf neurons showed multiple phases: nAChRs apparently mediated the fast and short inward current, M1 and/or M3 receptor may have mediated the fast and medium current, and the slow and long-lasting inward current was probably mediated by M3 and/or M5 receptors. Multiphasic excitatory cholinergic responses have been recorded in other CNS neurons. In the CL, short-lasting nicotinic and long-lasting muscarinic depolarizing responses were reported (Curro Dossi et al. 1991). nAChR-mediated fast excitatory cholinergic responses that were associated with a decrease in R_{in} were reported in the cat thalamic neurons (McCormick and Prince 1987) and in the rat superior colliculus (Sooksawate et al. 2008). A mAChR-mediated long-lasting depolarization was recorded in the guinea pig cerebral cortex, along with an increase in R_{in} (McCormick and Prince 1986). In the rat lateral geniculate nucleus, the M1 receptor was reported to mediate slow excitatory cholinergic responses with an increase in R_{in}, whereas the M3 receptor was presumed to be involved in the fast response with a decrease in R_{in} (Zhu and Uhlrich 1998). In our study, a R_{in} decrease was associated with the activation of all CAR-induced inward currents; however, this decrease in R_{in} was relatively small compared with that occurring during CAR-induced outward currents (5–20% of decrease for inward current, 50–70% of decrease for outward current). The opening of nonselective cation channels caused by activation of nAChRs may contribute to the R_{in} decrease in those Pf cells in which PRZ was not able to completely block the CAR-induced inward current. However, for those neurons whose inward current was completely blocked by PRZ or in the presence of MEC, the cause of the R_{in} decrease is unclear. M1 receptor activation has been previously reported to inhibit potassium and calcium currents (Gulledge and Stuart 2005; Liu et al. 2006; Uchimura and North 1990), which should theoretically increase R_{in}. However, it was also found that M1 receptor activation can induce a Ca^{2+}-dependent cation current largely permeable to Na^+ (Klink and Alonso 1997), and R-type Ca^{2+} channels can be enhanced by M1 receptor activation (Tai et al. 2006). Therefore one of the possible explanations for the muscarinic receptor-mediated R_{in} decrease is that different species and nuclei recruit distinct ionic mechanisms. Another reason may be the possible involvement of M3 or M5 receptors, whose transduction mechanisms remain uncertain. Also, the concentration-dependent selectivity of PRZ between M1 and M3 receptors for slice recordings is still controversial. In the available literature, the concentration used to block M1 receptors ranges from 25 nM to 10 μM. In our study, we used 10 μM PRZ, so that it is uncertain how selective this concentration is for M1 receptors specifically in the Pf.

A fast inhibitory followed by a delayed and long-lasting excitatory biphasic cholinergic response appeared only in 6.8% of recorded Pf neurons, which raised difficulties in identifying the specific subtypes of cholinergic receptors responsible for the biphasic response. We chose to test the nonselective muscarinic receptor antagonist, ATR. In an early report (McCormick and Prince 1987), such a biphasic cholinergic response appeared to be caused by the activation of muscarinic receptors. Previous studies of the detailed mechanism underlying fast inhibitory followed by slow excitatory cholinergic responses provide two plausible explanations. One is that the mAChR-mediated excitation of GABAergic neurons are presynaptic to the recorded cell (McCormick and Prince 1986). However, that study was conducted under current-clamp conditions, acetylcholine was pressure applied, and the inhibitory response recorded was sensitive to TTX. Even though TTX decreased the amplitude of outward currents more than the inward currents in our study, a detectable fast inhibitory phase still persisted in the presence of TTX. Moreover, we recorded in voltage-clamp mode, and CAR was superfused. Under these conditions, cholinergic modulation of presynaptic GABA release should be manifested as an increase in the frequency of IPSCs instead of a prolonged outward current. The second possible explanation for the biphasic cholinergic response was provided by another study that showed that CAR induced fast inhibitory responses via the transient activation of M1 receptors, which induced Ca^{2+} release from intracellular stores and subsequently activated Ca^{2+}-dependent K^+ channels (Gulledge and Stuart 2005). However, this does not offer a plausible interpretation for our results, because we only recorded this biphasic response in 6.8% of neurons, whereas 31.1% were excited by CAR, most likely via activation of M1 receptors. In addition, the manner in which we applied CAR was not "transient." Therefore the biphasic response was more likely induced by simultaneous activation of inhibitory (M2 and/or M4) and excitatory (M1, M3, and/or M5) muscarinic receptors, which may have distinct activation dynamics.

M2 receptors were found to occasionally co-localize with nAChRs in our study. However, the inhibitory effect of M2 receptors appeared to predominate over the excitatory effects of nAChRs, which were only detected when M2 receptors were blocked (n = 3). This may be because of the fast desensitization characteristic of nAChRs or because M2 receptors may be more somatic or proximal, whereas nAChRs may be more dendritic or distal.

Distinct membrane properties and functional implications

Typical TC neurons respond to synaptic inputs in a bursting or tonic mode and modulate rhythmic oscillations that may determine the cortical states (Llinas and Steriade 2006; Weyand et al. 2001), and these depend on low-threshold T-type Ca^{2+} channels and I_h currents (Jahnsen and Llinas 1984b). In our study, we did not pharmacologically distinguish LTS or I_h, but we quantified the density of rebound and of I_h current. The rebound current seems to be a combination of LTS and I_h, the activation of which by hyperpolarization induces bursting in TC neurons during SWS. In the Pf, cells that were excited or showed biphasic response to CAR had significantly higher density of rebound and I_h currents, so that in this aspect, these neurons may act more like typical TC neurons. However, a reduction or complete absence of LTS, as well as single-spike activity instead of bursting, has been reported in most Pf neurons recently (Lacey et al. 2007; Phelan et al. 2005). Our study confirmed this observation and extended it by determining that Pf neurons with these properties were inhibited by CAR. Moreover, Pf cells that were inhibited by CAR showed higher R_{in}, higher AP threshold, and longer AP half-width duration than that of CAR-excited neurons, suggesting that the excitability of the CAR-inhibited Pf neurons is lower than that of CAR-excited cells and probably lower than typical TC and CL neurons. These data indicate that cholinergic input to the Pf may differentially affect distinct populations of neurons that exhibit different electrophysiological properties.

Spontaneous or CAR-induced spikelets, which are rhythmic, subthreshold excitatory potentials thought to reflect firing in electrically coupled neurons, were recorded in a small group of Pf cells. In the thalamus, electrical synapses are thought to be mainly present among GABAergic nRt neurons and modulate synchronized rhythmic thalamocortical oscillations, and these neurons are more likely to be inhibited by cholinergic input (Deleuze and Huguenard 2006; Fuentealba and Steriade 2005). Recently, it was reported that electrical synapses represent a novel mechanism for sleep-wake control (Garcia-Rill et al. 2007, 2008). Our study discovered the potential presence of electrical coupling in the Pf, and more interestingly, all Pf neurons exhibiting spikelets showed excitatory cholinergic responses. Future studies need to be performed to confirm the presence of electrical coupling in the Pf by performing dual recordings, using fast synaptic blockers to isolate coupling, using QX-314 intracellularly to block dendritic sodium channels, and gap junction blockers to reduce or eliminate spikelets (Garcia-Rill et al. 2008). If these putative electrically coupled Pf neurons indeed are excited by cholinergic input, synchronized firing or oscillations would be produced, which may modulate cortical arousal and vigilance. Even though it is too early to conclude that all putative coupled Pf neurons are excited by cholinergic input, we can at least suggest these Pf neurons responded similarly to cholinergic input.

Development of cholinergic responses and membrane properties

Between postnatal days 10 and 30, a sharp decrease in REM sleep occurs in the rat, declining from >75% of total sleep time to ~15% of sleep time by 30 days of age (Jouvet-Mounier et al. 1970). A parallel developmental REM sleep decrease occurs in the human from birth to about 15 yr of age (Roffwarg et al. 1966) and was observed in the first 2 wk after birth in the kitten (Chase and Sterman 1967). It has been suggested that there is a REM sleep inhibitory process that develops during the first 2 wk of life in the rat (Vogel et al. 2000). This model predicts that one or more inhibitory processes may become progressively stronger during this period, and stimulation or blockade of this process will decrease or increase the manifestations of REM sleep, respectively. A disturbance of the developmental decrease in REM sleep has been proposed to result in a life-long increase in REM sleep drive and hypervigilance such as that observed in a number of disorders that have a mostly postpuberty age of onset (Feng et al. 2001; Kobayashi et al. 2004b). Our previous studies found that, in the PPN, mAChR, 5-HT1, and $GABA_A$ receptor–mediated inhibition showed a significant developmental increase. However, few studies have investigated the developmental changes in intrinsic membrane properties and synaptic interactions in the thalamus, which modulates different rhythmic oscillations in distinct sleep-wake states. This study found that Pf neurons are more likely to be inhibited by cholinergic input later in development; however, early in development, the chances of being inhibited or excited are almost equal. However, in typical "specific" TC neurons, excitatory cholinergic responses seem to be predominant in the rest of the thalamus (Curro Dossi et al. 1991; McCormick 1992; McCormick and Prince 1987; Zhu and Uhlrich 1998) and produce high-frequency tonic firing during waking and REM sleep. We postulate that the developmental change in cholinergic responses in the Pf may be one of the proposed REM sleep inhibitory processes, but it needs to be further confirmed by experiments in adult Pf cells, which current whole cell patch-clamp methods cannot accomplish. A previous report using extracellular recordings of adult Pf neurons following electrical stimulation of the PPN showed a predominant excitatory response, whereas only ~20% of cells were inhibited (Capozzo et al. 2003). However, this does not imply that cholinergic responses of adult Pf neurons are mainly excitatory, because we recently found that noncholinergic PPN neurons, including glutamatergic and GABAergic cells, send efferent projections to the Pf as well (unpublished data).

On the other hand, the stereotypical electrophysiological features of classical "specific" TC neurons, such as rebound current/LTS and I_h currents, tend to decrease with development in the Pf. These data suggest that at least some Pf neurons may transition from a typical "specific" TC type of neuron to a distinct one with development. The reduction of rebound current and I_h in Pf neurons means these cells have lower potential for bursting activity such as "specific" TC neurons or CL cells do when hyperpolarized. We suspect that Pf neurons participate in the modulation of REM sleep together with other TC cells in early development, when REM sleep is predominant and less specific synaptic interactions may be required. Whereas, later in development, their function may be focused on sensory processing and involved in selective attention during wakefulness and the transition from sleep to waking. However, the mechanisms underlying these transitions and the change of cholinergic responses across age remain unclear. The developmental changes in membrane properties and cholinergic responses of Pf cells may represent two independent processes. The increase in inhibitory cholinergic responses could be caused by the upregulation of M2 receptors, changes

in potassium channel expression, or alterations in intracellular signal pathways. The decrease in the density of rebound current and I_h may be directly attributable to the decrease in the expression of I_h and calcium channels or to changes in membrane properties, which further affect the dynamics of these currents. Further studies are needed to dissect out the exact mechanisms, but our results open a new avenue for understanding the maturation of thalamocortical interactions, as well as their associated physiological functions.

In addition to the change in cholinergic responses and decreases in rebound and I_h currents, R_{in}, AP half-width duration in Pf neurons, and the proportion of cells with spikelets also decreased with development. The developmental changes in these intrinsic membrane properties seem to parallel the changes that occur in other central nervous neurons during maturation (Garcia-Rill et al. 2007; Heister et al. 2007; Kobayashi et al. 2004a; Yao and Xiong 2005). From this aspect, CAR-excited Pf neurons seem to mature earlier than inhibited cells.

In summary, cholinergic input from the brain stem mesopontine region to the thalamus plays a very important role in the modulation of cortical arousal and sleep-wake cycles by depolarizing TC neurons and hyperpolarizing nRt (Hobson and Pace-Schott 2002; Pace-Schott and Hobson 2002). Our results show, however, that cholinergic inputs exert predominantly inhibitory effects on Pf neurons, especially later in development, and perhaps in the adult. The developmental changes in membrane properties of Pf neurons and their cholinergic responses suggest a transition from typical TC neuron-like activity to a distinct one, indicating a fundamentally different function.

GRANTS

This work was supported by National Institute of Health Grants DC-07123, NS-20246, and RR-20146.

REFERENCES

Allen TG, Brown DA. M2 muscarinic receptor-mediated inhibition of the Ca^{2+} current in rat magnocellular cholinergic basal forebrain neurones. *J Physiol* 466: 173–189, 1993.

Capozzo A, Florio T, Cellini R, Moriconi U, Scarnati E. The pedunculopontine nucleus projection to the parafascicular nucleus of the thalamus: an electrophysiological investigation in the rat. *J Neural Transm* 110: 733–747, 2003.

Chase MH, Sterman MB. Maturation of patterns of sleep and wakefulness in the kitten. *Brain Res* 5: 319–329, 1967.

Curro Dossi R, Pare D, Steriade M. Short-lasting nicotinic and long-lasting muscarinic depolarizing responses of thalamocortical neurons to stimulation of mesopontine cholinergic nuclei. *J Neurophysiol* 65: 393–406, 1991.

Deleuze C, Huguenard JR. Distinct electrical and chemical connectivity maps in the thalamic reticular nucleus: potential roles in synchronization and sensation. *J Neurosci* 26: 8633–8645, 2006.

Deschenes M, Bourassa J, Doan VD, Parent A. A single-cell study of the axonal projections arising from the posterior intralaminar thalamic nuclei in the rat. *Eur J Neurosci* 8: 329–343, 1996a.

Deschenes M, Bourassa J, Parent A. Striatal and cortical projections of single neurons from the central lateral thalamic nucleus in the rat. *Neuroscience* 72: 679–687, 1996b.

Endoh T. Muscarinic M2 receptor inhibition of calcium current in rat nucleus tractus solitarius. *Neuroreport* 18: 1141–1145, 2007.

Erro E, Lanciego JL, Gimenez-Amaya JM. Relationships between thalamostriatal neurons and pedunculopontine projections to the thalamus: a neuroanatomical tract-tracing study in the rat. *Exp Brain Res Exp Hirnforschung* 127: 162–170, 1999.

Feng P, Ma Y, Vogel GW. Ontogeny of REM rebound in postnatal rats. *Sleep* 24: 645–653, 2001.

Fuentealba P, Steriade M. The reticular nucleus revisited: intrinsic and network properties of a thalamic pacemaker. *Prog Neurobiol* 75: 125–141, 2005.

Garcia-Rill E, Charlesworth A, Heister D, Ye M, Hayar A. The developmental decrease in REM sleep: the role of transmitters and electrical coupling. *Sleep* 31: 673–690, 2008.

Garcia-Rill E, Heister DS, Ye M, Charlesworth A, Hayar A. Electrical coupling: novel mechanism for sleep-wake control. *Sleep* 30: 1405–1414, 2007.

Gulledge AT, Stuart GJ. Cholinergic inhibition of neocortical pyramidal neurons. *J Neurosci* 25: 10308–10320, 2005.

Heister DS, Hayar A, Garcia-Rill E. Differential effects of carbachol on dorsal subcoeruleus neurons. *Neurosci* 735.25, 2007.

Henderson JM, Carpenter K, Cartwright H, Halliday GM. Loss of thalamic intralaminar nuclei in progressive supranuclear palsy and Parkinson's disease: clinical and therapeutic implications. *Brain* 123: 1410–1421, 2000.

Hobson JA, Pace-Schott EF. The cognitive neuroscience of sleep: neuronal systems, consciousness and learning. *Nat Rev Neurosci* 3: 679–693, 2002.

Ito S, Craig AD. Vagal-evoked activity in the parafascicular nucleus of the primate thalamus. *J Neurophysiol* 94: 2976–2982, 2005.

Jahnsen H, Llinas R. Electrophysiological properties of guinea-pig thalamic neurones: an in vitro study. *J Physiol* 349: 205–226, 1984a.

Jahnsen H, Llinas R. Ionic basis for the electro-responsiveness and oscillatory properties of guinea-pig thalamic neurones in vitro. *J Physiol* 349: 227–247, 1984b.

Jouvet-Mounier D, Astic L, Lacote D. Ontogenesis of the states of sleep in rat, cat, and guinea pig during the first postnatal month. *Dev Psychobiol* 2: 216–239, 1970.

Kha HT, Finkelstein DI, Pow DV, Lawrence AJ, Horne MK. Study of projections from the entopeduncular nucleus to the thalamus of the rat. *J Comp Neurol* 426: 366–377, 2000.

Klink R, Alonso A. Ionic mechanisms of muscarinic depolarization in entorhinal cortex layer II neurons. *J Neurophysiol* 77: 1829–1843, 1997.

Kobayashi S, Nakamura Y. Synaptic organization of the rat parafascicular nucleus, with special reference to its afferents from the superior colliculus and the pedunculopontine tegmental nucleus. *Brain Res* 980: 80–91, 2003.

Kobayashi T, Good C, Biedermann J, Barnes C, Skinner RD, Garcia-Rill E. Developmental changes in pedunculopontine nucleus (PPN) neurons. *J Neurophysiol* 91: 1470–1481, 2004a.

Kobayashi T, Good C, Mamiya K, Skinner RD, Garcia-Rill E. Development of REM sleep drive and clinical implications. *J Appl Physiol* 96: 735–746, 2004b.

Lacey CJ, Bolam JP, Magill PJ. Novel and distinct operational principles of intralaminar thalamic neurons and their striatal projections. *J Neurosci* 27: 4374–4384, 2007.

Liu L, Zhao R, Bai Y, Stanish LF, Evans JE, Sanderson MJ, Bonventre JV, Rittenhouse AR. M1 muscarinic receptors inhibit L-type Ca^{2+} current and M-current by divergent signal transduction cascades. *J Neurosci* 26: 11588–11598, 2006.

Llinas R, Jahnsen H. Electrophysiology of mammalian thalamic neurones in vitro. *Nature* 297: 406–408, 1982.

Llinas RR, Steriade M. Bursting of thalamic neurons and states of vigilance. *J Neurophysiol* 95: 3297–3308, 2006.

McCormick DA. Cellular mechanisms underlying cholinergic and noradrenergic modulation of neuronal firing mode in the cat and guinea pig dorsal lateral geniculate nucleus. *J Neurosci* 12: 278–289, 1992.

McCormick DA, Prince DA. Mechanisms of action of acetylcholine in the guinea-pig cerebral cortex in vitro. *J Physiol* 375: 169–194, 1986.

McCormick DA, Prince DA. Actions of acetylcholine in the guinea-pig and cat medial and lateral geniculate nuclei, in vitro. *J Physiol* 392: 147–165, 1987.

Minamimoto T, Kimura M. Participation of the thalamic CM-Pf complex in attentional orienting. *J Neurophysiol* 87: 3090–3101, 2002.

Pace-Schott EF, Hobson JA. The neurobiology of sleep: genetics, cellular physiology and subcortical networks. *Nat Rev Neurosci* 3: 591–605, 2002.

Phelan KD, Mahler HR, Deere T, Cross CB, Good C, Garcia-Rill E. Postnatal maturational properties of rat parafascicular thalamic neurons recorded in vitro. *Thalamus Relat Syst* 3:2: 89–113, 2005.

Raeva SN. The role of the parafascicular complex (CM-Pf) of the human thalamus in the neuronal mechanisms of selective attention. *Neurosci Behav Physiol* 36: 287–295, 2006.

Roffwarg HP, Muzio JN, Dement WC. Ontogenetic development of the human sleep-dream cycle. *Science* 152: 604–619, 1966.

Sooksawate T, Isa K, Isa T. Cholinergic responses in crossed tecto-reticular neurons of rat superior colliculus. *J Neurophysiol* 100: 2702–2711, 2008.

Steriade M, Datta S, Pare D, Oakson G, Curro Dossi RC. Neuronal activities in brain-stem cholinergic nuclei related to tonic activation processes in thalamocortical systems. *J Neurosci* 10: 2541–2559, 1990.

Steriade M, McCormick DA, Sejnowski TJ. Thalamocortical oscillations in the sleeping and aroused brain. *Science* 262: 679–685, 1993.

Tai C, Kuzmiski JB, MacVicar BA. Muscarinic enhancement of R-type calcium currents in hippocampal CA1 pyramidal neurons. *J Neurosci* 26: 6249–6258, 2006.

Uchimura N, North RA. Muscarine reduces inwardly rectifying potassium conductance in rat nucleus accumbens neurones. *J Physiol* 422: 369–380, 1990.

Van der Werf YD, Witter MP, Groenewegen HJ. The intralaminar and midline nuclei of the thalamus. Anatomical and functional evidence for participation in processes of arousal and awareness. *Brain Res Brain Res Rev* 39: 107–140, 2002.

Vogel GW, Feng P, Kinney GG. Ontogeny of REM sleep in rats: possible implications for endogenous depression. *Physiol Behav* 68: 453–461, 2000.

Weyand TG, Boudreaux M, Guido W. Burst and tonic response modes in thalamic neurons during sleep and wakefulness. *J Neurophysiol* 85: 1107–1118, 2001.

Williams JA, Comisarow J, Day J, Fibiger HC, Reiner PB. State-dependent release of acetylcholine in rat thalamus measured by in vivo microdialysis. *J Neurosci* 14: 5236–5242, 1994.

Yan W, Zhang QJ, Liu J, Wang T, Wang S, Liu X, Chen L, Gui ZH. The neuronal activity of thalamic parafascicular nucleus is conversely regulated by nigrostriatal pathway and pedunculopontine nucleus in the rat. *Brain Res* 1240: 204–212, 2008.

Yao XH, Xiong Y. Changes in electrophysiological and morphological properties of neuron in the ventral partition of medial geniculate body during the postnatal development of rats. *Sheng Li Xue Bao* 57: 333–339, 2005.

Zhu JJ, Uhlrich DJ. Cellular mechanisms underlying two muscarinic receptor-mediated depolarizing responses in relay cells of the rat lateral geniculate nucleus. *Neuroscience* 87: 767–781, 1998.